WHC-SA--1392-Rev.1

DE92 008367

Comparison of Fracture Behavior for Low-Swelling Ferritic and Austenitic Alloys Irradiated in the Fast Flux Test Facility (FFTF) to 180 DPA

F. H. Huang

Date Published
February 1992

To Be Published in
Engineering Fracture Mechanics

Prepared for the U.S. Department of Energy
Assistant Secretary for Nuclear Energy

Westinghouse Hanford Company
P.O. Box 1970
Richland, Washington 99352

Hanford Operations and Engineering Contractor for the
U.S. Department of Energy under Contract DE-AC06-87RL10930

Approved for Public Release

COMPARISON OF FRACTURE BEHAVIOR FOR LOW-SWELLING FERRITIC AND AUSTENITIC ALLOYS IRRADIATED IN THE FAST FLUX TEST FACILITY (FFTF) TO 180 DPA

F. H. Huang
Westinghouse Hanford Company, Richland, WA 99352, U.S.A.

ABSTRACT

Fracture toughness testing was conducted to investigate the radiation embrittlement of high-nickel superalloys, modified austenitic steels and ferritic steels. These materials have been experimentally proven to possess excellent resistance to void swelling after high neutron exposures. In addition to swelling resistance, post-irradiation fracture resistance is another important criterion for reactor material selection. By means of fracture mechanics techniques the fracture behavior of those highly irradiated alloys was characterized in terms of irradiation and test conditions. Precipitation-strengthened alloys failed by channel fracture with very low postirradiation ductility. The fracture toughness of titanium-modified austenitic stainless steel D9 deteriorates with increasing fluence to about 100 displacement per atom (dpa), the fluence level at which brittle fracture appears to occur. Ferritic steels such as HT9 are the most promising candidate materials for fast and fusion reactor applications. The upper-shelf fracture toughness of alloy HT9 remained adequate after irradiation to 180 dpa although its ductile-brittle transition temperature (DBTT) shift by low temperature irradiation rendered the material susceptible to brittle fracture at room temperature. Understanding the fracture characteristics under various irradiation and test conditions helps reduce the potential for brittle fracture by permitting appropriate measures to be taken.

INTRODUCTION

The mechanical properties of core components in advanced reactors will be degraded by large fluxes of fast neutron and energetic charged particles; it is therefore of vital interest to search continuously for improved alloys for these components and test them in hostile environments. Neutron bombardment of the materials causes swelling, creep and embrittlement problems. Void swelling and irradiation creep lead to the dilation and bowing of reactor core components and limit the achievable burn-ups in the fuel. These dimensional instability may create overstress or overheating, indirectly resulting in failure.

Of great concern is the radiation embrittlement caused by high neutron exposure. The lifetime of the core components depends mostly on the degree of embrittlement they suffered. Emphasis has been placed on swelling reduction improvements since austenitic steels first used in fast reactors applications were found to swell 30 percent at 400 °C. Subsequent reactor experiments have shown that high nickel superalloys [1], titanium (Ti)-modified austenitic steels [2] and ferritic/martensitic steels [3] all exhibit less than 1 percent increase in volume after high fluence irradiation. As the dose has recently accumulated up to 230 dpa in the Fast Flux Test Facility (FFTF) in Richland, Washington, it is important to investigate the extent of radiation embrittlement for these materials. Tensile testing, though simple and economical, is not a reliable method for radiation embrittlement studies because the flawed structures may fail catastrophically at a stress level much lower than the yield stress, and the ductility becomes less sensitive to a change in irradiation conditions in high fluence environments.

The need to assess radiation-induced toughness degradation is met best by fracture mechanics techniques. The efforts of those involved in developing fracture mechanics techniques have made available reasonably accurate fracture test methods. Linear elastic fracture mechanics (LEFM) has been employed to evaluate the severity of a crack in a structure. In the case where the structure does not exhibit linear elastic behavior, the large plastic strain developed around the crack tip prevents LEFM from being applied. A plasticity correction term is then introduced, and elastic-plastic fracture mechanics (EPFM) is used to characterize the ductile fracture behavior.

EPFM techniques were used to evaluate the fracture toughness of reactor materials and subsized compact tension specimens were preferred, as reactor core components were thin (on the order of a few millimeters) and usually fail by ductile fracture. Irradiation space saving and temperature gradient reduction are other reasons for using small specimens. However, reducing specimen size for irradiated materials without jeopardizing data validity is not straightforward. The effect of specimen size on fracture toughness has been investigated [4]. To perform the irradiation experiments, test specimens were prepared from material stocks of interest and placed in the FFTF for irradiation or cut from reactor components with desired irradiation conditions. Test results obtained from various highly irradiated alloys exhibiting superior swelling resistance were analyzed by means of fracture mechanics techniques. Suggestions will be made about which material is suitable for use in high neutron fluence environments and worth further efforts.

EXPERIMENTAL PROCEDURE

Specimen Preparation

Compact tension specimens were prepared from alloys D66 (high-nickel superalloy), D9 (Ti-modified austenitic steel) and HT9 (ferritic/martensitic steel). Table 1 lists the chemical compositions of these alloys. Two types of compact tension specimen were tested in this work: a disk-shaped and a rectangular specimen. The 2.54-mm thick and 16-mm diameter disk-shaped specimens were machined from 2.8-mm-thick rolled stock of D66 and D9, and from 3.2-mm-thick stock formed from 33.3 mm diameter bar stock of HT9 (heat No.91353 and 84425). The final heat treatment for HT9 was 1038 °C/5 min/AC + 760 °C/30 min/AC.

The D66 specimens were irradiated in the Experimental Breeder Reactor-II (EBR) to a fluence of 2.7×10^{22} n/cm^2 and HT9 specimens in the FFTF to a fluence of 38.5×10^{22} n/cm^2 (equivalent to about 180 dpa for HT9). The preirradiation toughness and crack propagation resistance were so low that none of the irradiated D66 specimens was tested.

Compact tension specimens were also cut from a 3-mm thick FFTF duct of D9 which had been irradiated to a peak fluence of 23.5×10^{22} ($E > 0.1$ MeV). The duct was fabricated by Clark and Wheeler from heat no. N562. The specimen had a width of 12.7 mm; the dimensions of compact tension specimen are in Ref. 5. Alloy D9 is a Ti-modified AISI 316 stainless steel (316 SS) and swells only a little compared to 316 SS. All specimens of D66, D9 and HT9 were tested by means of the single-specimen electric-potential method. Four steel electrodes were welded to each specimen to make the connection of electrical leads in the hot cell easier.

Test Procedure

The test procedure was not much different from that reported earlier [5]. Postirradiation K_{Ic} and J_{Ic} fracture toughness tests were performed at 30, 205, and 410 °C in accordance with the test procedures outlined in ASTM E339 and E813, respectively. Before testing, each specimen was fatigue precracked to an a/w ratio of approximately 0.55 by the electric potential technique to monitor the crack length. To insulate the test specimen assembly electrically, ceramic spacers were placed in the couplings of the pull rods. During each test, the load, electric potential output, and displacement were recorded continuously. After the test was completed, each cracked specimen was heat tinted at 400 °C to reveal the crack extension.

The specimen used in irradiated testing was more than one hundred times smaller than the one recommended in the ASTM standards, but three types of fracture behavior were observed to result from fracture degradation following irradiation: (1) unstable fracture -- the loading curve was a straight line up to the maximum load and the electric potential increased suddenly at the maximum load as shown in Figure 1; (2) stable tearing followed by unstable fracture -- the loading curve displayed some plastic deformation up to the maximum load followed by the rapid decline of the load while the electric-potential increased drastically before reaching the maximum load as shown in Figure 2; (3) stable tearing -- both load and potential output increased smoothly up to the maximum load; the load then decreased gradually while the potential output continued to increase as shown in Figure 3.

Fractography

Fractographic examination was performed using a scanning electron microscope (Model JSM-35C) operating at 25 keV. To minimize personnel radiation exposure, a sliver of material containing the fracture surfaces was sectioned from tested samples using an acid saw.

RESULTS

Alloy D66

Load and potential output versus displacement curves of unirradiated D66 are shown in Figure 4. The electric potential curve deviated abruptly in the region of crack initiation and then extended upward smoothly. The values of J_{Ic} were obtained from D66 specimens tested at 25 and 232 °C. Type 2 fracture behavior was obtained for D66 samples that were not exposed to neutron irradiation. The low values of fracture toughness and tearing modulus listed in Table 2 and plotted in Figures 5 and 6 indicate that D66 has weak fracture resistance. This characteristic was consistent with fractography that showed D66 fractured by flow localization with channel facets on the fracture surface. More on this subject will be discussed later.

Alloy D9

Two high fluence samples cut from the D9 duct failed during fatigue precracking at stress intensity levels of about 12-14 MPa$\sqrt{m}$. The third one, tested without precracking, failed by unstable brittle fracture without plastic deformation (Figure 1). The fracture toughness of this unprecracked specimen was over-estimated because the notch tip in the specimen was blunt.

The specimens cut from the lower fluence (9-10 x 10^{22} n/cm^2) section of the D9 duct exhibited stable tearing. The equivalent K_{1c} computed from J_{1c}, termed as K_c, are given in Table 2. For D9 specimens irradiated to a fluence of 10 x 10^{22} n/cm^2 and tested at 410 °C, Type 2 fracture behavior was observed (Figure 3). Results are plotted in Figure 7 as a function of test temperature; also plotted in the figure are fracture toughness data for 316 SS irradiated to a fluence of 16 x 10^{22} n/cm^2. Evidently, the postirradiation toughness of D9 decreased slightly with increasing test temperature and was inferior to that of 316 SS.

The values of the tearing modulus for D9 samples are also given in Table 2 and plotted in Figure 6, which shows that the crack propagation resistance in D9 was reduced significantly after irradiation.

Alloy HT9

All HT9 samples tested displayed stable tearing. Load and potential output curves for HT9 irradiated to a fluence as high as 38.5 x 10^{22} n/cm^2 are shown in Figure 8. The values of K_c and T are listed in Table 2 and plotted in Figures 9 and 10. Results showed that the fracture toughness value of HT9 irradiated to a high fluence of 38.5 x 10^{22} n/cm^2 was greater than 100 MPa$\sqrt{m}$. For HT9 irradiated to a fluence of 14 x 10^{22} n/cm^2 at 550 °C, the toughness (122 MPa$\sqrt{m}$) was slightly larger than that of HT9 samples cut from the FFTF duct that was irradiated to 16 x 10^{22} n/cm^2 at 411° [5]. Overall, the present data proved that the fracture toughness of HT9 remained adequate when the material was irradiated at temperatures at 400 °C or higher.

DISCUSSION

Fracture Mechanism

Alloy D66

In nickel and its solid-solution alloys, ductility troughs were observed decades ago in the neighborhood of 600 °C [6]. The fracture mode changes from a low-temperature ductile fracture to a high-temperature brittle intergranular fracture as the temperature increases from approximately half the absolute melting temperature. It changes because at high temperature, cavities are nucleated and grow as grain boundaries slide significantly. High-temperature intergranular embrittlement also results from the grain boundary segregation because the presence of impurities on the grain boundaries reduces the energy absorption in fracture.

The extremely low ductilities of the precipitation-strengthened alloys after irradiation are believed to be caused by the precipitation of γ'(Ni_3Si or Ni_3Al) near or along the grain boundaries [7]. The γ' precipitates developed during the double-aged treatment for D66 contribute the high strength of the alloy but also induce slip in confined regions, or channels, during deformation. Alloy D66 was fractured by flow localization as indicated by the presence of channel facets on the fracture surface (Figure 11). This type of failure is analogous to the channel fracture of irradiated stainless steels first observed by Fish et al. [8].

Alloy D9

The scanning electron microscope (SEM) fractographs for unirradiated and irradiated 20 percent CW 316 SS were compared in Ref. 9. After irradiation the facets generated by a shear process on the fracture surfaces of 20 percent

cold worked (CW) 316 SS replaced the transgranular plastic dimpling feature. The fracture surface morphologies of D9 are believed to be little different from 20 percent CW 316 SS. Large amounts of channel fracture are expected in D9 duct samples irradiated to 22 x 10^{22} n/cm^2. Irradiation causes dislocation channeling, which creates defect-free channels resulting in channel fracture morphology [8]. Irradiation at 400 to 482 °C in alloy D9 produces $\gamma'(Ni_3Si)$ and η(Cr-Ni-Silicide). These phases become obstacles to the movement of dislocation; a larger force therefore is required for dislocation to pass through these phases, and this process results in an increase in yield stress for irradiated D9. Voids and Frank loops also contribute to the yield stress increase. A high yield strength alloy like irradiated D9 tends to exhibit poor toughness because the resistance to slip is so high that the fracture stress is reached before plastic deformation can occur.

Alloy HT9

The fracture process observed in HT9 irradiated to a fluence of 5.5 x 10^{22} n/cm^2 changed little with fluence [10]. As shown in Figure 12a, the fracture surfaces of highly irradiated HT9 were characterized by ductile dimpling through microvoid coalescence. These fracture surfaces are in contrast to the plate-like faceted fracture surfaces of high-nickel superalloys or irradiated austenitic steels. However, stable tearing would change to cleavage fracture behavior if the HT9 were irradiated at 360 °C and tested at room temperature (Figure 12b). The flatness of the facets and irregular cleavage steps with river patterns are visible in this figure. These are evident fractographic features for cleavage fracture. Fine scale precipitates such as G-phase, a face-centered cubic (fcc) nickel silicide, and

dislocation loops formed during irradiation at low temperatures are believed to cause a large amount hardening. The critical stress for cleavage fracture can be reached at a higher temperature, thus raising the ductile-brittle transition temperature (DBTT) [11].

In body-centered cubic (bcc) structures such as HT9 there exists a large energy barrier in lattice to dislocation slip; the materials are likely to fail through low-index crystallographic planes without significant plastic deformation. Both cleavage and channel fracture are the worst cases of fracture and always catch the engineer by surprise. While scientists are still unable to prevent channel fracture from occurring in austenitic alloys, the cleavage fracture can be avoided simply by increasing irradiation or handling temperature [5]. Figures 12a and 12b show that the fracture feature was altered from dimpling rupture at 205 °C to cleavage facet at room temperature for FFTF duct samples irradiated at 360 °C. High temperature softens the hardening in ferritic steels resulting from irradiation, and reduces the shear strength, which becomes smaller than the cohesive strength; thus the crack will blunt plastically before it can initiate and propagate.

Subsized Specimen for Postirradiation Testing

For reasons mentioned in the previous sections, small specimens have more advantages over large specimens for postirradiation fracture testing with electric potential techniques. The electric potential techniques are capable of revealing the rapid crack initiation and propagation for the second type of fracture behavior, stable tearing followed by unstable fracture. Experimental evidence has shown that reasonably accurate plane strain fracture toughness can be obtained from specimens of various sizes if the specimen size criteria

recommended in ASTM E399 are satisfied. In the present study, highly irradiated D9 samples with a thickness of 2.54 mm and the K_{1c} values of about 22 MPa$\sqrt{m}$ or lower should satisfy the thickness criterion: $2.5(K_Q/\sigma_y)^2$. As the specimens exhibited linear elastic behavior, the other requirements for valid data should also be met.

Requirements for the validity of fracture toughness data obtained from specimens exhibiting stable tearing are more complicated because stable tearing depends on a "data exclusion zone" (DEZ) size for J_{1c} determination. While initiation fracture toughness is not specimen-size dependent, in maintaining J-controlled conditions the DEZ size is. The minimum thickness ($25J_{1c}/\sigma_y$) required for valid J_{1c} values is satisfied by the 1.02-mm-thick specimens of 20 percent CW 316 SS and the 2.54-mm-thick specimens of D9, as a result of low toughness and irradiation hardening. To compare the fracture responses of different materials to irradiation, the procedure for J_{1c} determination needs to be consistent for all subsized samples of various materials.

Irradiated Effect On Fracture Resistance

The iron-nickel base precipitation-strengthened alloys have been long noted for their superior high-temperature strength and resistance to radiation-induced void swelling. The development of the family of these alloys for use in fast reactors was an important part of the National Cladding/Duct Materials Development Program beginning in 1974 [12]. However, it soon was found that the commercial alloy Nimonic PE16 exhibited zero ductility after neutron irradiation [13]. A great number of superalloy specimens in the shape of miniaturized transmission electron microscope (TEM)

disks with different composition and thermomechanical treatments (TMT), irradiated to fluences of 4.7 to 7.6 x 10^{22} n/cm^2, were available for mechanical property testing. Therefore, a quick screening test capable of measuring the ductility or toughness of these irradiated disk specimens was urgently needed. In 1978, a bend-test technique was developed at Westinghouse Hanford Company to permit rapid screening of irradiated disk specimens. The results had not been released by the time the test technique was reported in the open literature [14] in 1982. Table 3 lists some of those results for TEM disk specimens of six commercial and four developmental superalloys, along with the composition, irradiation and test conditions. The severe radiation embrittlement exhibited by specimens of all commercial as well as developmental alloys dashed the hope that the problems might be improved by varying composition and TMT.

Fracture toughness testing was performed on unirradiated superalloys D66 and D21 and on irradiated D21. Although D21 has the best toughness compared to other superalloys, it exhibited stable tearing/unstable fracture behavior and poor crack propagation resistance [15]. The low fracture toughness resulting from channel fracture and high-temperature intergranular fracture is the common feature for all high-strength precipitation-strengthened alloys. These phenomena also occur in highly irradiated austenitic stainless steels.

The effects of irradiation on the fracture toughness of 20 percent cold-worked 316 SS were reported in References 9 and 16. The radiation embrittlement problems found in 316 SS are expected to occur in alloy D9. In comparison, the toughness at the maximum load of irradiated D9[2] was lower than that of irradiated 316 SS at temperatures above 200 °C. Channel fracture features were also observed in D9 under high neutron fluence. On the basis of

these results, it is not certain whether the lowest fluence that causes channel fracture in alloy D9 will be higher than that which causes the similar embrittlement in 316 SS, as previously was thought. The fracture toughness values of both alloys are plotted as a function of fluence in Figure 13. The figure shows that the fracture toughness degraded with fluence and that D9 may fail by brittle fracture at fluences near 20 x 10^{22} n/cm^2. Charpy test results show a correlation between swelling and embrittlement in cold worked Ti-modified 316 SS [17]. D9 exhibits lower swelling at fluences about 15 to 20 x 10^{22} n/cm^2. Thus, D9 may have better resistance to radiation embrittlement than 316 SS, based on Charpy tests.

Unlike austenitic steels, ferritic steels not only can suppress void swelling but also remain tough under high neutron fluence. Figure 14 shows the 410 °C fracture toughness in terms of fluence; also plotted in the figure is the toughness data for D9. The fracture toughness of HT9 seemed to saturate with fluence, while D9 exhibited toughness that declined rapidly as the fluence was increased and failed by brittle fracture at fluences above 20 x 10^{22} n/cm^2. At fluences about 10 to 12 x 10^{22} n/cm^2, once the crack in D9 initiated, fast fracture followed; and the crack propagation resistance was very low, as indicated by the tearing modulus in Figure 15. The fracture mode in D9 changed from Type 3 (stable tearing) to Type 2 (stable tearing-unstable fracture) and ended as Type 1 (unstable fracture) as the fluence increased. In contrast to alloy D9, HT9 displayed a Type 3 fracture mode that was not altered by irradiation. The tearing modulus decreased with increasing fluence, but remained high even at fluences above 30 x 10^{22} n/cm^2.

The results showing that HT9 had a high fracture resistance to irradiation were somewhat surprising, as the material had been known to be susceptible to a ductile-brittle transition at a temperature (DBTT) that shifted upward with irradiation. The DBTT shift apparently was not changed significantly by neutron fluence. However, fracture toughness testing on a section of an FFTF duct from below a fuel column [5] revealed that HT9 irradiated at 360 °C exhibited low fracture toughness and failed by brittle fracture at room temperature. The effects of irradiation on the mechanical properties of specimens from the center region of the FFTF duct (irradiation temperature = 419-445 °C) and the lower region (irradiation temperature = 360 °C) are quite different. Apparently, irradiation temperature is the key factor in the degree of radiation embrittlement for ferritic steels. The important findings from these studies were the following: (a) the low-temperature irradiated fracture samples of HT9 failed without plastic deformation despite the fact that the tensile specimens of the same conditions exhibited 10 percent elongation. This finding indicated that fracture toughness testing is necessary to detect the potential for brittle fracture; (b) Increasing test temperature may increase the fracture toughness of the low-temperature irradiated HT9 with fracture mode changing from cleavage to dimpling. This finding suggested that the brittle problems of ferritic steels may be alleviated by raising the handling or irradiation temperatures cautiously. For austenitic steels, the embrittlement concerns of channel fracture will not likely diminish.

Fast And Fusion Reactor Applications

The swelling problem for austenitic stainless steels was reduced by varying the composition of the material, but the radiation-induced embrittlement remained a major problem for the high-exposure performance of austenitic steels in advanced reactors. Moreover, although D9 exhibits excellent swelling resistance at fluences around 10 x 10^{22} n/cm^2, it loses its superiority in suppressing swelling to 316 SS as the fluence increases to 36.9 x 10^{22} n/cm^2 (Table 4). Clearly, the use of alloy D9 should be limited to around 20 x 10^{22} n/cm^2; caution therefore should be taken in dealing with the potential risk of sudden failure for D9 components exposed to beyond this fluence range.

In addition to the superior fracture toughness under large neutron fluence, HT9 was found to swell only 0.3 percent at a fluence as high as 32.9 x 10^{22} n/cm^2 (about 160 dpa) compared to 30 percent for D9 which has good swelling resistance at much lower fluences (see Table 4). This high resistance to radiation-induced swelling is inherent in ferritic steels (bcc alloys) and is explained as the consequence of the trapping of radiation-induced point defects by interstitial and substitutional solutes [18]. The significant effects of trapping on precipitation result in the phase stability in bcc materials under high neutron fluences [19].

Because the poor-toughness superalloys were not considered and the use of Ti-modified austenitic steels may have to be limited to about 100 dpa, ferritic steels emerge as the most promising candidate materials for fast and fusion reactor applications, especially for the fusion first wall, which has to withstand 40 MW-y/m^2 neutron irradiation (a displacement damage of approximately 480 dpa for ferritic steels). Experimental results in this work

have shown that no material other than ferritic steels are likely to satisfy these irradiation requirements. In the future attention will focus on the assessment of low-irradiation temperature effects on toughness and on the improvement of high-temperature strength for these materials. An understanding of fracture behavior in terms of irradiation temperature and fluence for ferritic steels, based on a wide series of in- and ex-reactor experiments, can build confidence in the use of these materials for fast and fusion reactor applications.

CONCLUSIONS

The radiation embrittlement of low-swelling alloys, high-nickel superalloys, austenitic steels and ferritic steels has been assessed using fracture mechanics techniques. The fracture toughness test results lead to the following observations.

- The fracture toughness of HT9 remains adequate after irradiation with fluences up to 180 dpa at temperatures of 400 °C or higher. Irradiation temperatures have a strong effect in degrading the fracture toughness for HT9, but results show that the fracture mode of low-temperature irradiated HT9 changes from cleavage fracture to dimpling rupture when the temperature is increased.

- The potential for brittle failure exists for austenitic steel D9 when irradiated to fluences above 20 x 10^{22} n/cm^2 (E > 0.1 MeV). The fracture toughness of D9 was found to deteriorate with increasing fluence. Samples irradiated to 23 x 10^{22} n/cm^2 fail by brittle fracture without plastic deformation. This embrittlement is associated with channel fracture similar to that observed in highly irradiated 316 SS.

- Bend-test results of TEM disks show that high-nickel superalloys exhibit extremely low ductility after irradiation as a result of precipitation that occurs in narrow bands during deformation. The pre-irradiation fracture toughness of D66 is low, and the material is fractured by flow localization with the fracture surfaces characterized by channel facets.

- Subsized specimens are suitable for in-cell fracture toughness testing for irradiated materials. Use of electric potential techniques causes the irradiated 2.5 to 3.0-mm-thick specimens to display different fracture modes ranging from linear elastic behavior to stable tearing depending upon the fracture responses to irradiation. Size requirements for data validity are satisfied by all irradiated subsized specimens.

- Analysis of the fracture property values obtained by fracture mechanics techniques, together with fracture mode observation and fracture surface morphologies, provides the best method for studying the radiation embrittlement of nuclear structure materials under large neutron exposures. The results obtained in this work indicated that the service of low-swelling austenitic steels should be limited to displacement damage levels of approximately 100 dpa and that ferritic steels are the most promising candidate materials for extended high-temperature service in fast reactors and for fusion reactor applications in very high neutron fluence environments.

ACKNOWLEDGMENTS

This paper is based work performed under U.S. Department of Energy Contract DE-AC06-87RL10930 with Westinghouse Hanford Company, a subsidiary of Westinghouse Electric Corporation.

REFERENCES

[1] W. G. Johnston, T. Lauritzen, J. H. Rosolowski and A. M. Turakalo, An experimental survey of swelling in commercial Fe-Cr-Ni alloys bombarded with 5 MeV Ni ions. *J. Nuclear Mater.* 54, 24-40 (1974).

[2] B. J. Makenas, Swelling of 316 stainless steel and D9 cladding in FFTF. *Radiation-Induced in Microstructure.* ASTM STP 955, 146-153 (1987).

[3] D. S. Gelles, Microstructural examination of several commercial ferritic alloys irradiated to high fluence. *J. Nuclear Mater.* 103 and 104, 975-979 (1981).

[4] F. H. Huang and D. S. Gelles, Influence of specimen size and microstructure on the fracture toughness of a martensitic stainless steel. *Engng Fracture Mech.* 19, 1-20 (1984).

[5] F. H. Huang, Fracture toughness and tensile properties of alloy HT9 in thin sections under high neutron fluence. *Effects of Radiation on Materials*, the 15th symposium, Nashville, Tennessee, ASTM STP 1125 (1990).

[6] *Nickel and Its Alloys*, section J, International Nickel Company, New York, 5-7 (1947).

[7] W. J. S. Yang, Grain boundary segregation in solution-treated Nimonic PE16. *J. Nuclear Mater.* 108 and 109, 339-346 (1982).

[8] R. L. Fish, J. L. Straalsund, C. W. Hunter and J. J. Holmes, Swelling and tensile property evaluations of high-fluence EBR-II thimbles. *Effects of Radiation on Substructure and Mechanical Properties of Metals and Alloys.* ASTM STP 529, 149-164 (1973).

[9] F. H. Huang, The fracture characterization of highly irradiated Type 316 stainless steel. *Int. J. Fracture* 25, 181-193 (1983).

[10] F. H. Huang, Fracture behavior of irradiated HT9 for structural applications. *Nuclear Engng. Design* 90, 13-23 (1985).

[11] W. L. Hu and D. S. Gelles, The ductile-to-brittle transition behavior of martensitic steels neutron irradiated to 26 dpa. *Influence of Radiation on Material Properties*. ASTM STP 956, 83-97 (1987).

[12] J. J. Laidler, J. J. Holmes and J. W. Bennett, U.S. program on reference and advanced cladding/duct materials. *Radiation Effects in Bredder Reactor Structural Materials*. TMS/AIME, 41-52 (1977).

[13] R. Bajaj, R. P. Shogan, C. DeFlitch, R. L. Fish, M. M. Paxton and M. L. Bleiberg, Tensile properties of neutron irradiated Nimonic PE16. *Effects of Radiation on Materials*. ASTM STP 725, 326-351 (1980).

[14] F. H. Huang, M. L. Hamilton and G. L. Wire. Bend testing for miniature disks. *Nuclear Tech.* 57, 234-242 (1982).

[15] F. H. Huang, Post-irradiation fracture properties of precipitation-strengthened alloy D21. *Influence of Radiation on Material Properties*. ASTM STP 956, 141-150 (1987).

[16] M. L. Hamilton, F. H. Huang, W. J. S. Yang and F. A. Garner, Mechanical properties and fracture behavior of 20% cold-worked 316 stainless steel irradiated to very high neutron exposures. *Influence of Radiation in Material Properties*. ASTM STP 956, 245-270 (1987).

[17] A. Fissolo, R. Cauvin, J. Hugot, and V. Levy, Influence of swelling on irradiated CW titanium 316 embrittlement. *Effects of Radiation on Materials*. ASTM STP 1046, 700-713 (1990).

[18] E. A. Little, Void-swelling in irons and ferritic steels, I, mechanisms of swelling suppression. *J. Nuclear Mater.* 87, 11-24 (1979).

[19] A. Wolfenden, J. R. Holland, R. G. Lott and J. A. Spitznagel, Phase

stability in irradiated bcc materials. *Phase Stability During Irradiation*. TMS-AIME, 383-413 (1982).

TABLE 1. CHEMICAL COMPOSITIONS.

Element	D66	HT9 (Heat No. 91353)	HT9 (84425)	D9 (N562)	D9 (2966)
Cr	12.0	11.97	11.87	13.5	14.06
Ni	45.0	0.57	0.53	16.07	15.60
Mo	3.0	1.03	1.02	1.5	1.45
V	-	0.33	0.30	<0.2	-
Si	0.5	0.22	0.27	0.97	1.05
Mn	-	0.49	0.58	1.7	2.3
C	0.03	0.21	0.2	0.048	0.043
Al	2.5	0.023	0.002	<0.05	0.05
Ti	2.5	0.002	<0.01	0.2	0.25
P	-	0.08	0.003	<0.02	0.011
S	-	0.03	0.004	<0.01	0.001
Co	-	0.01	0.011	<0.05	0.04
Cu	-	0.074	0.013	<0.04	0.03
B	0.005	0.001	0.001	<0.001	<0.001
W	-	0.52	0.55	-	-
As	-	<0.005	<0.005	<0.03	<0.01
N	-	0.004	0.0017	<0.01	0.007
Cb	-	-	-	<0.05	0.01
Ta	-	-	-	<0.02	<0.01
Zr	0.05	-	-	-	-
Fe	Bal.	Bal.	Bal.	Bal.	Bal.

TABLE 2. FRACTURE TOUGHNESS RESULTS FOR LOW-SWELLING ALLOYS.

Materials	Test Temp(°C)	Irrad. Temp(°C)	Fluence (10^{22} n/cm^2)	K_c (Mpa$\sqrt{m}$)	Tearing Modulus
D66	25	---	0	72.3	4
	232	---	0	74.2	4
D9 Duct	205	457	9	93.9	66
	410	455	10	70.8	18
	410	390	22.8	<30.1	0
	---	423	21.3	*	---
	---	430	20.0	**	---
D9(2966)	32	410	17.5	79.9	18
	205	410	20.9	61.4	4
	410	410	20.9	58.0	---
HT9(91353)	32	550	13	129.5	211
	205	550	13	101.6	146
	25	405	17.5	110.0	79
	205	405	17.5	108.9	80
	30	410	38.5	103.0	78
	205	410	38.5	96.4	70
	410	410	38.5	93.7	55
HT9(84425)	205	550	14	122.1	105
	410	550	14	97.4	137
	30	410	32.9	121.8	58
	205	410	32.9	110.6	79
	410	410	32.9	100.3	39

* Failed at 13.9 MPa$\sqrt{m}$ During Fatigue Precracking
** Failed at 12.4 MPa$\sqrt{m}$ During Fatigue Precracking

TABLE 3. DISK BEND-TEST RESULTS.

ALLOY	COMPOSITION	HEAT CODE	BEND DUCTILITY (%) T.T. = I.T. + 110 °C I.T. = 500	550	600
Nimonic PE16	Fe-34.0 Ni-43.5 Cr-16.5 Mo-3.3 Mn-0.1 Ti-1.2 Al-1.2 Si-0.2 Nb-0.05 C-0.05 B-0.01	1C	0.40	0.44	0.20
Inconel 706	Fe-37.0 Ni-41.5 Cr-16.0 Mo-0.1 Si-0.2 Mn-0.2 Ti-1.75 Al-0.2 Nb-2.9 C-0.03 B-0.001	7C	-	0.20	-
Inconel 718	Fe-18.6 Cr-19.0 Ni-52.5 Mo-3.0 Nb-5.1 Ti-0.9 Al-0.5 Si-0.1 Mn-0.18 C-0.04	7J	-	0.44	-
Incoloy 901	Fe-36 Ni-42.5 Cr-12.5 Mn-0.1 Mo-5.7 Ti-2.8 Al-0.2 C-0.05 Si-0.1 B-0.015	7P	-	0.14	-
A286	Fe-53 Cr-15 Ni-26 Mo-1.25 Ti-2.15 Al-0.2 Si-0.4 Mn-1.4 V-0.3 C-0.05	7R	-	0.78	-
M813	Fe-39 Cr-18 Ni-35 Mo-4 Ti-2.25 Al-1.4 C-0.08	7K	-	0.04	-

TABLE 3. DISK BEND TEST RESULTS (Cont.)

ALLOY	COMPOSITION	HEAT CODE	BEND DUCTILITY (%) T.T. = I.T. + 110 °C I.T. = 500	550	600
D42	Fe-19 Cr-15 Ni-60 Mo-5 Al-1.5 Ti-1.5 Nb-1.5 Si-0.5 B-0.01 Zr-0.03 C-0.03	BP	-	0.26	-
D66	Fe-34 Ni-45 Cr-12 Mo-3 Ti-2.5 Al-2.5 Si-0.5 Zr-0.05 B-0.005 C-0.03	LJ	0.40	0.60	-
		LN	-	-	0
D21	Fe-58.5 Ni-25 Cr-8.4 MO-1.0 Si-1.0 Mn-1.0 Ti-3.3 Al-1.7 Nb-0.05 C-0.04 B-0.001	LO	>0.50	0.61	0.81
		L3	-	-	0
D68	Fe-36 Ni-45 Cr-12 Mo-0.1 Si-0.4 Mn-0.3 Ti-1.8 Al-0.4 Mb-3.6 C-0.03 B-0.005	LV	-	-	0
		NC	-	-	0.16

TABLE 4. SWELLING DATA FOR 20% COLD WORKED 316 STAINLESS STEEL, D9 AND HT9

Specumen	Alloy	Heat No.	Irradiation Temp. (°C)	Fluence (10^{22} n/cm^2)	ΔV/V (%)
AB01	316 SS	93591	410	37.2	17.7
AB04	316 SS	93591	410	37.2	23.2
EF01	D9	83508	410	36.9	31.4
EF02	D9	83508	410	36.9	29.8
HK21	HT9	91353	550	13	0.03
HK22	HT9	91353	550	13	0.02
AN18	HT9	84425	410	32.9	0.22
AN20	HT9	84425	410	32.9	0.31

Figure 1. Load and Electric Potential Records for Unstable Fracture Behavior.

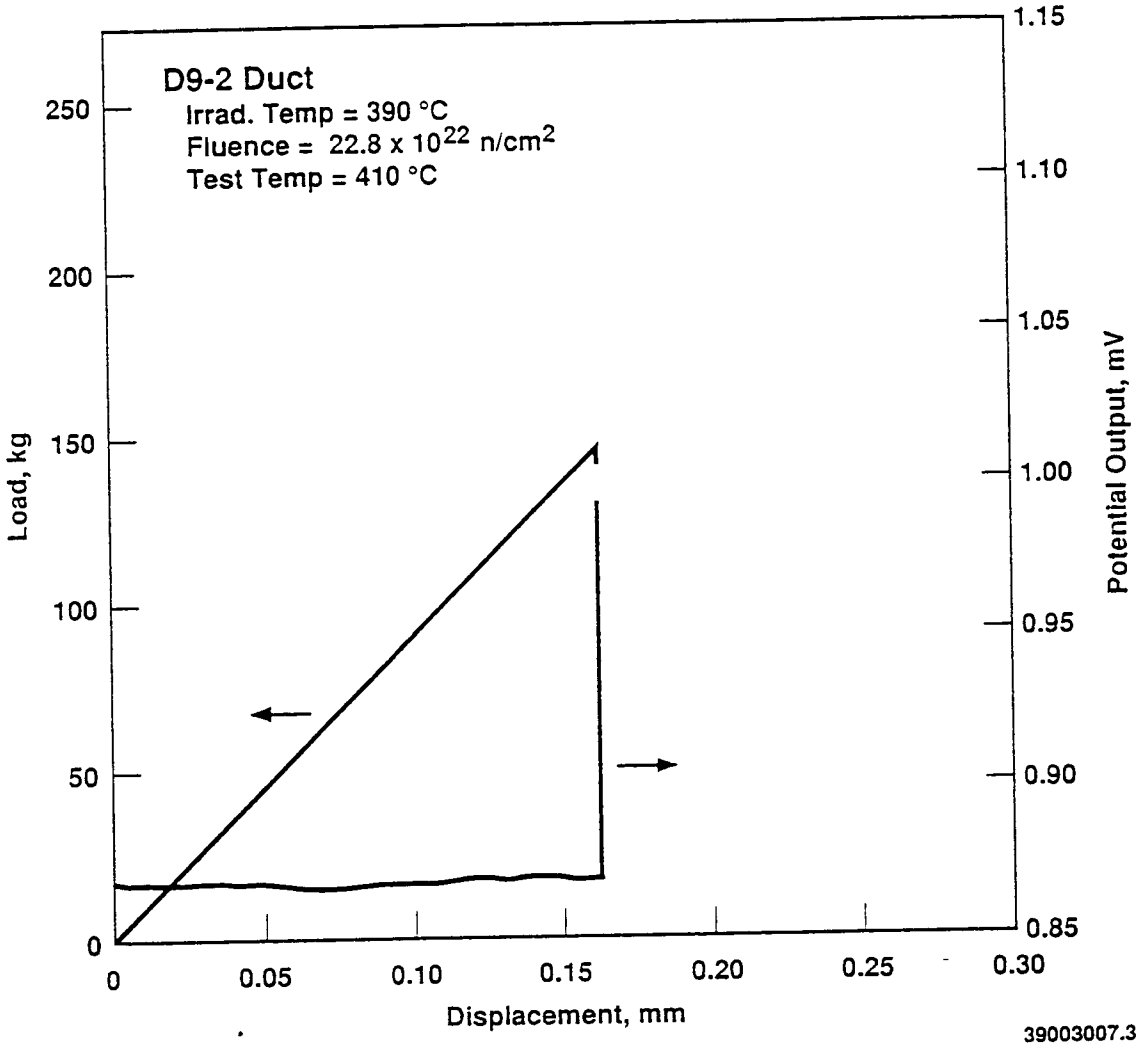

Figure 2. Load and Electric Potential Records for Stable/Unstable Fracture Behavior.

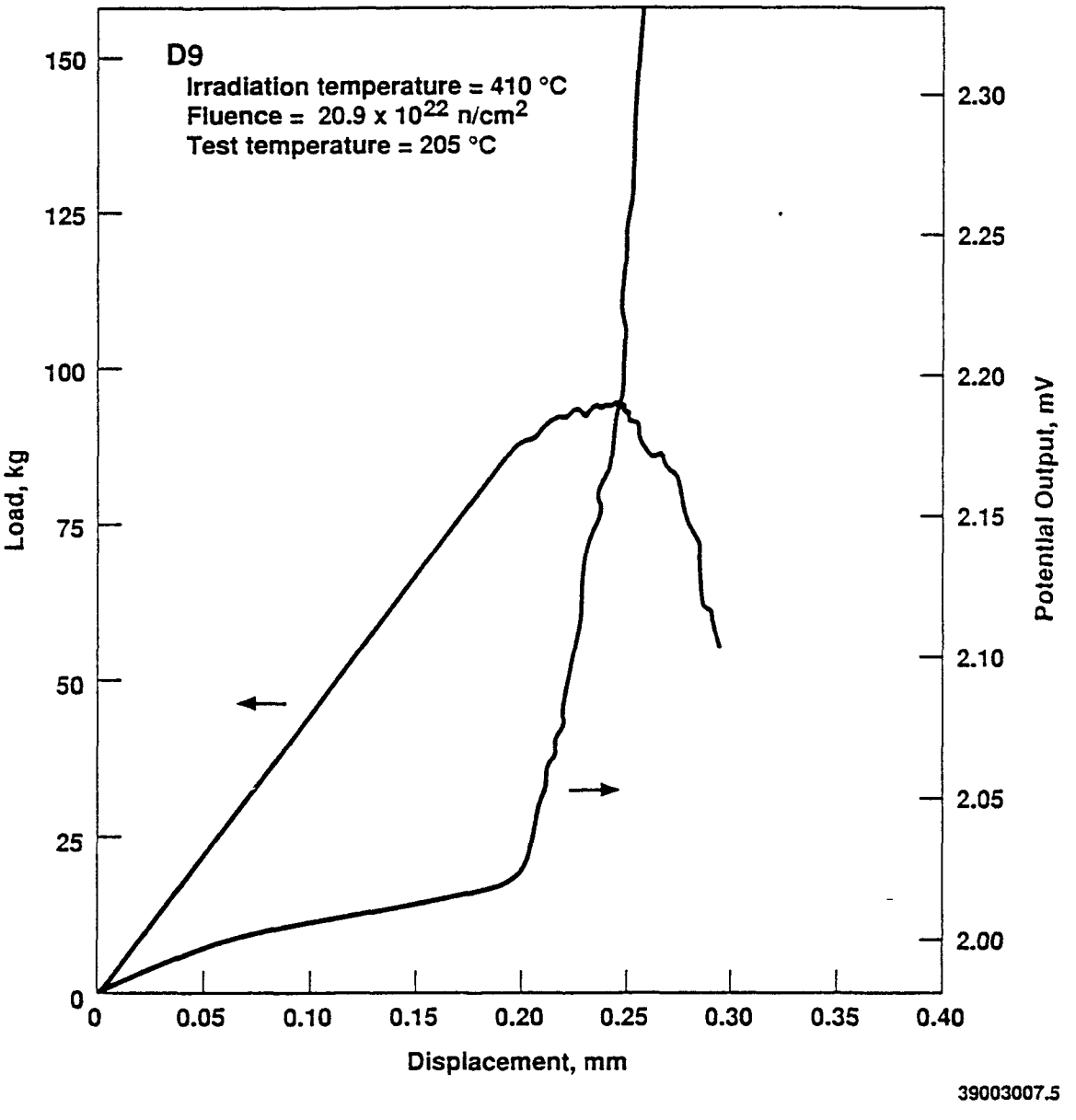

Figure 3. Load and Electric Potential Records for Stable Tearing Fracture Behavior.

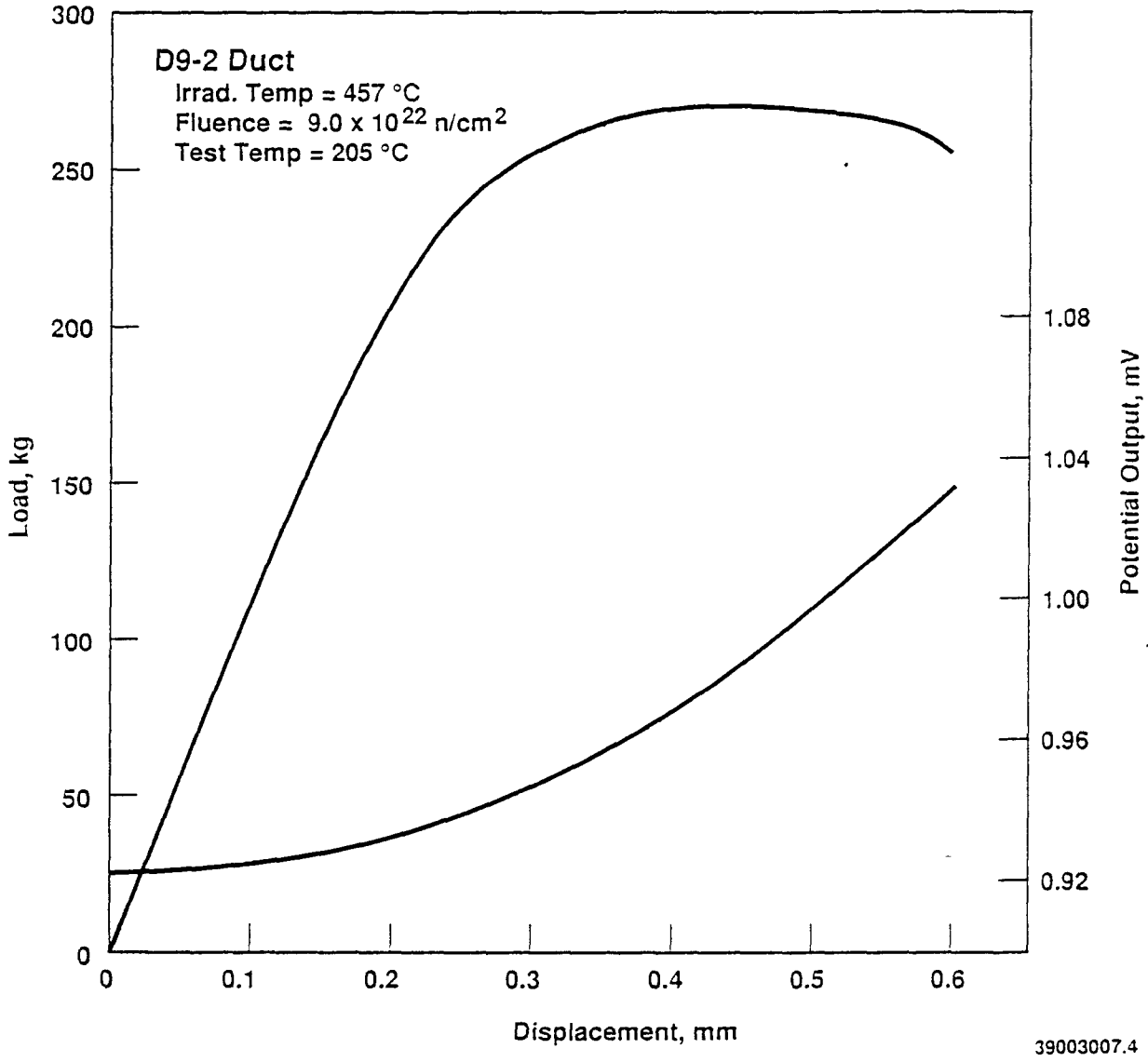

Figure 4. Load and Electric Potential Records for D66 Tested at 25 °C.

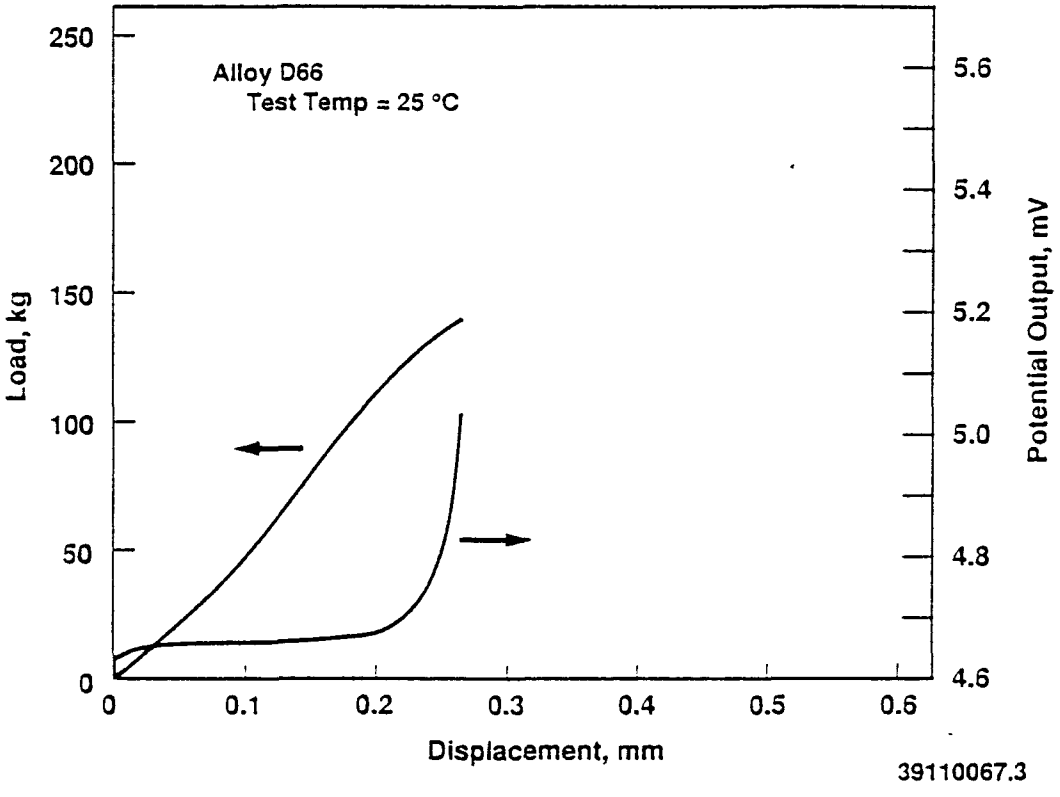

Figure 5. Temperature Dependence of Fracture Toughness for D21 and D66.

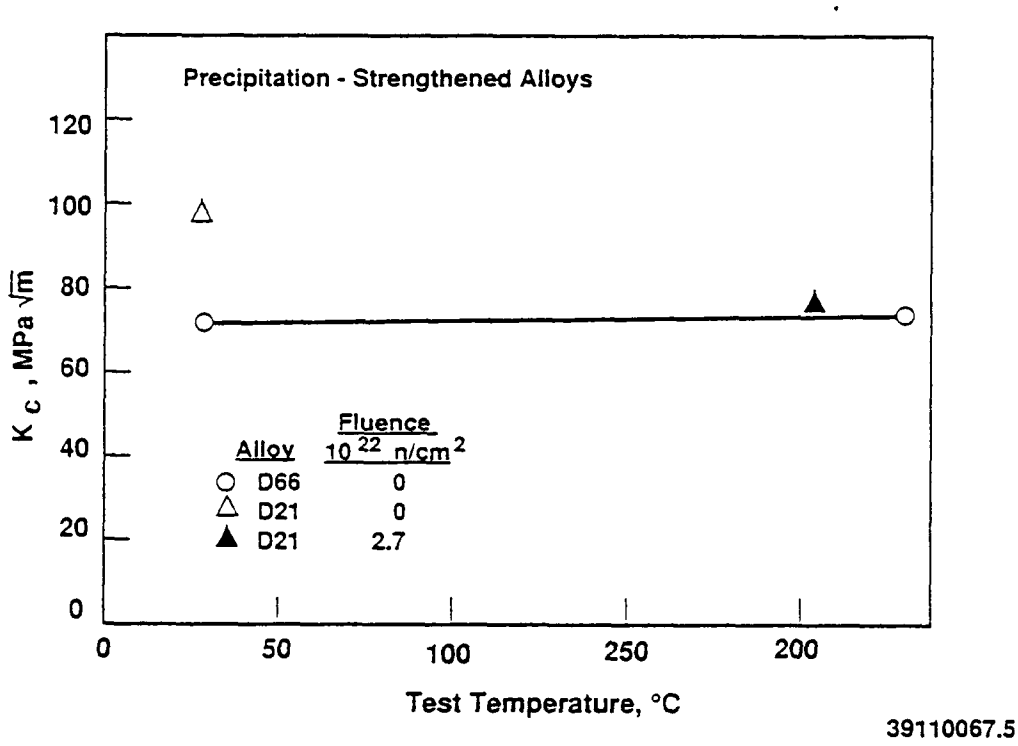

Figure 6. Temperature Dependence of Tearing Modulus for D21, D66 and D9.

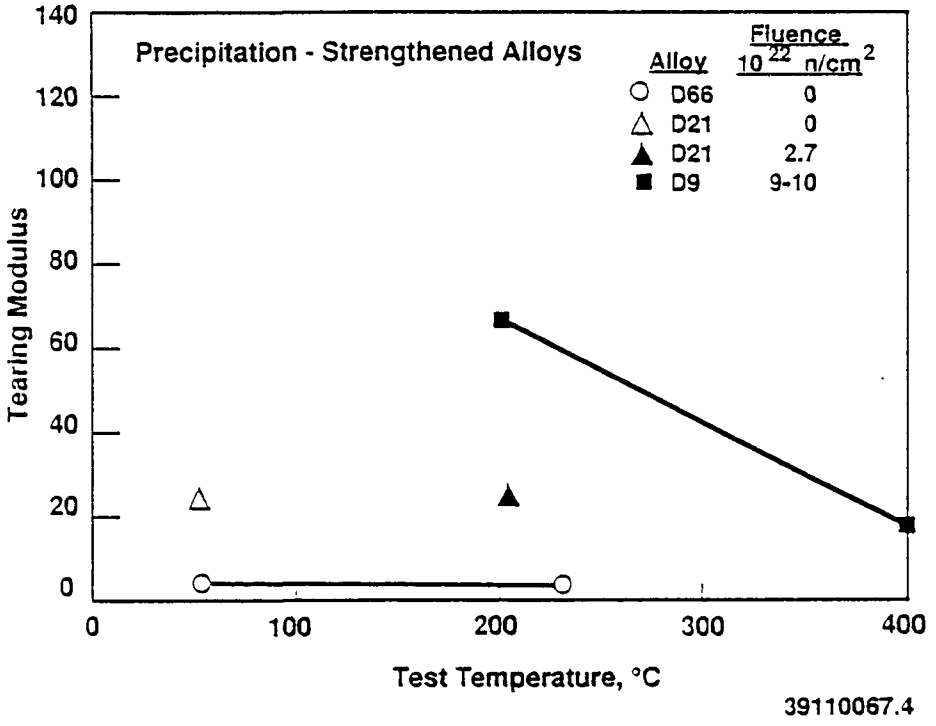

Figure 7. Temperature Dependence of K_c or K_{max} for Irradiated D9.

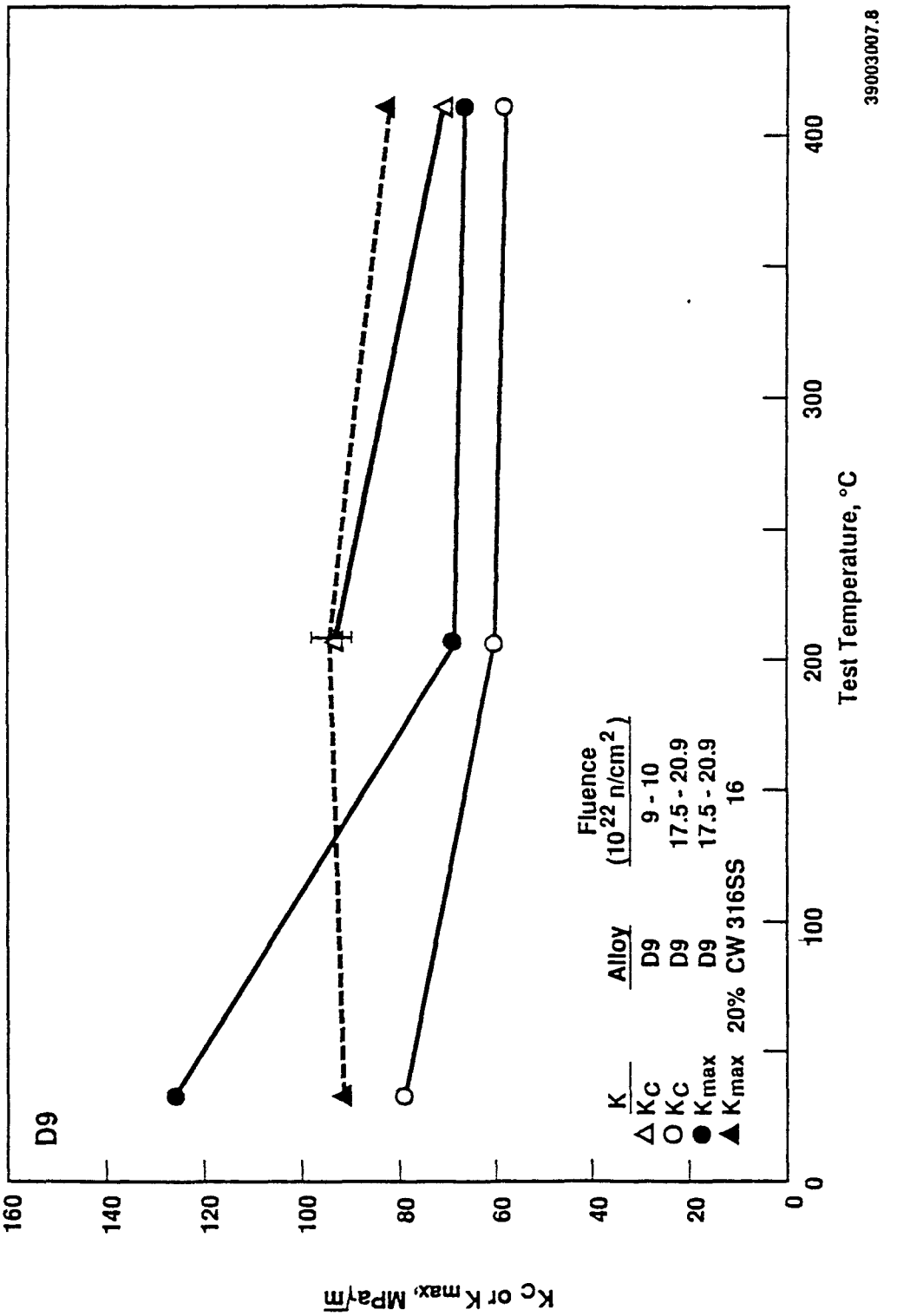

Figure 8. Load and Electric Potential Records for HT9 Irradiated to 38.5 x 10^{22} n/cm^2.

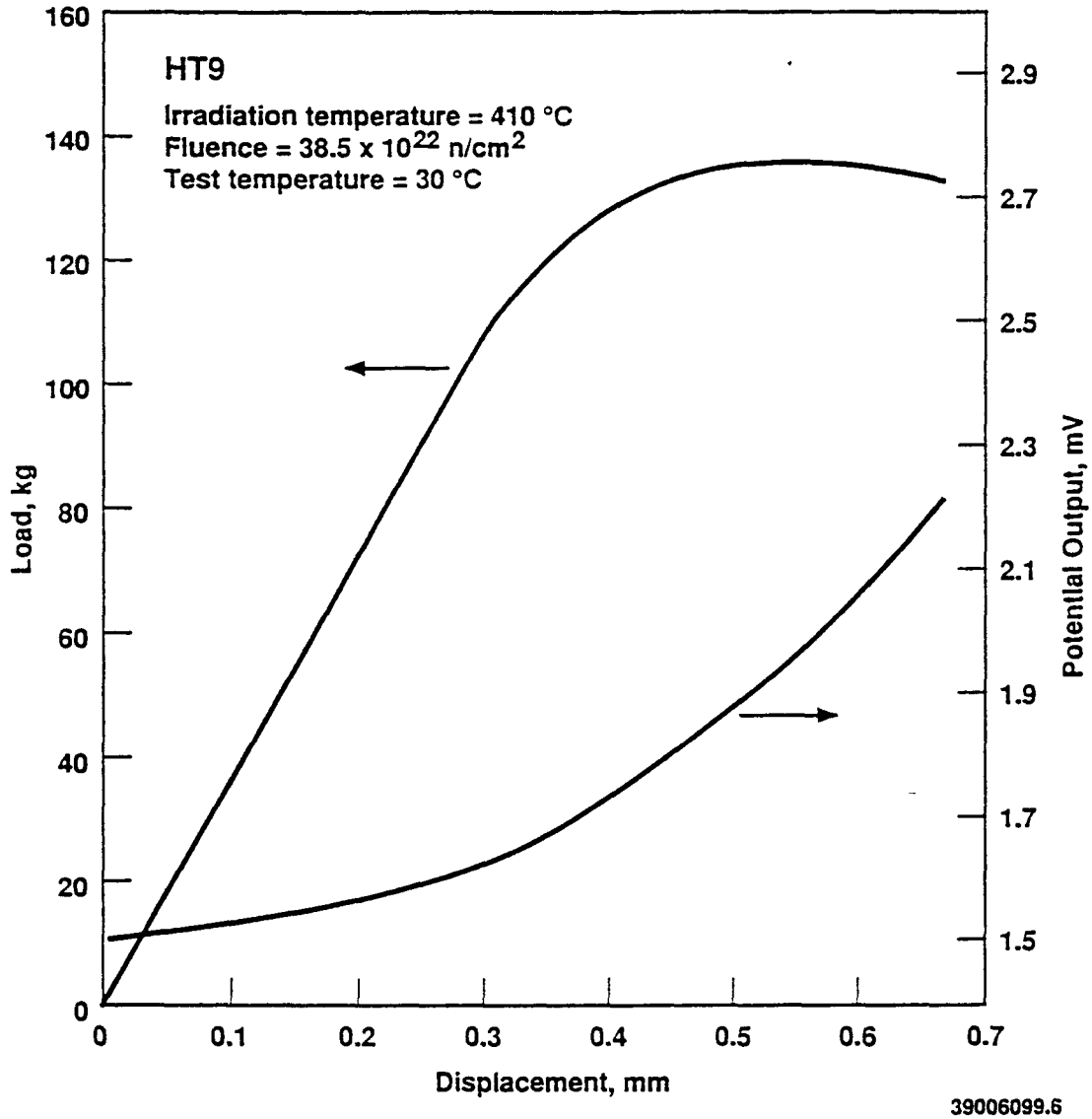

Figure 9. Temperature Dependence of Fracture Toughness for Irradiated HT9.

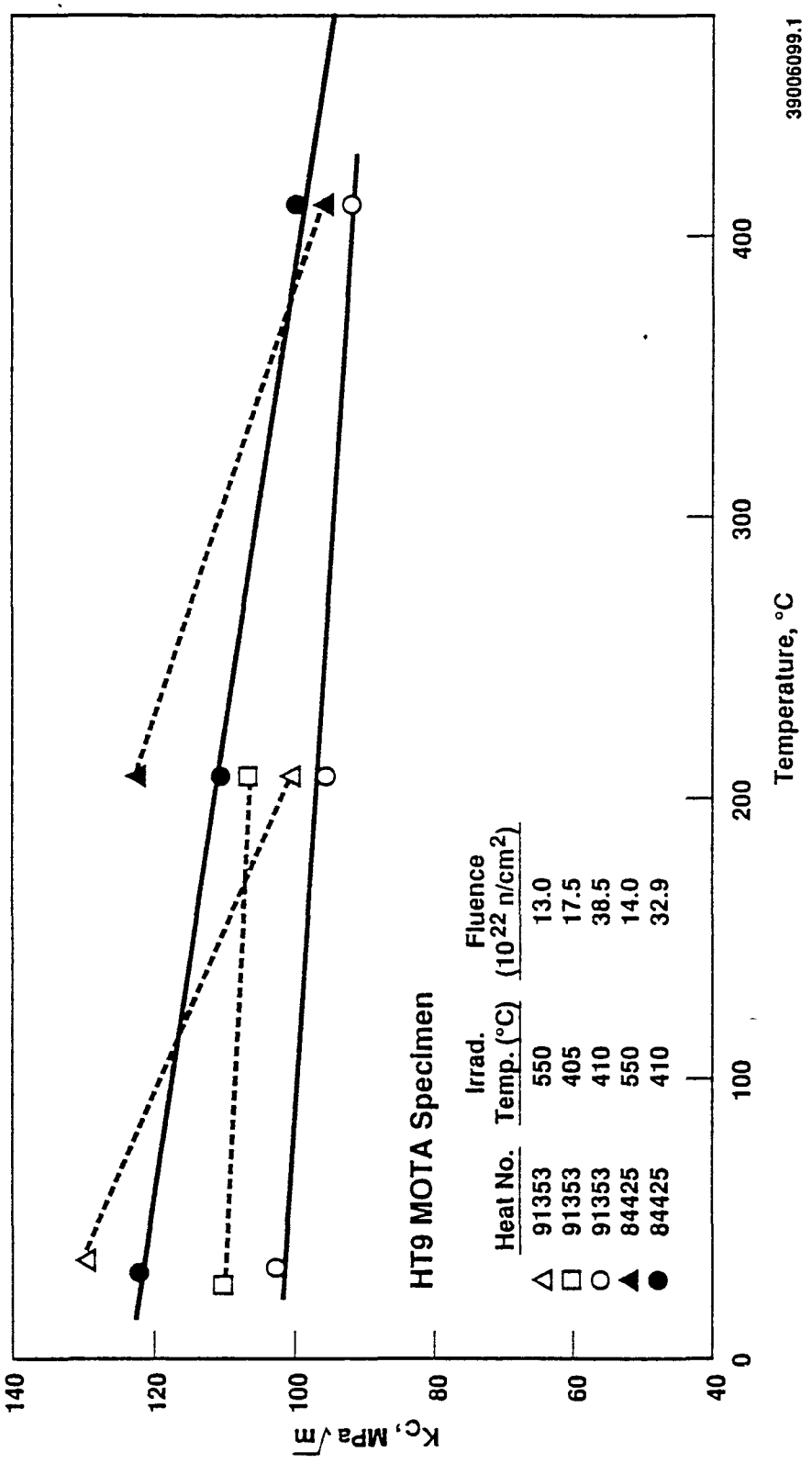

Figure 10. Temperature Dependence of Tearing Modulus for Irradiated HT9.

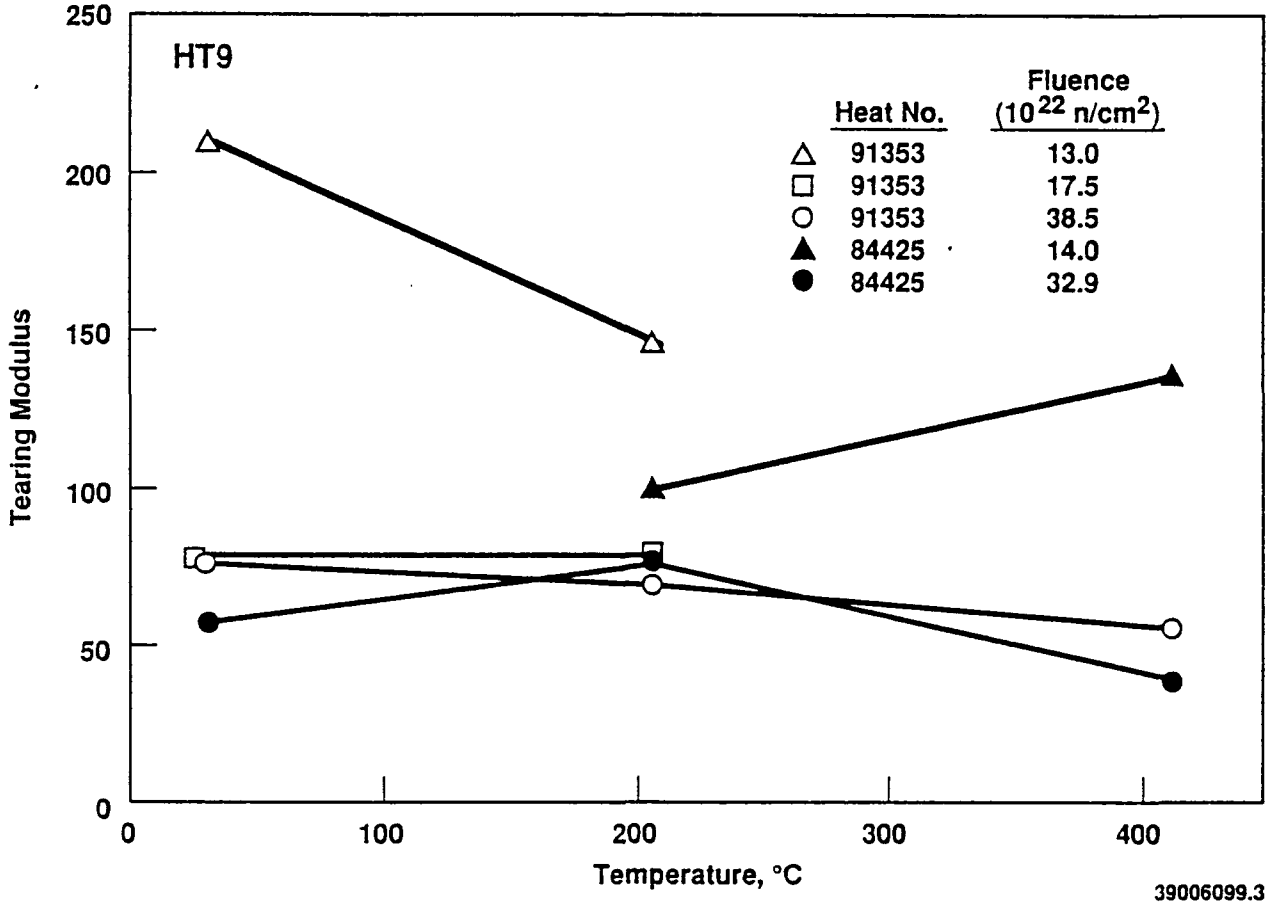

Figure 11. Scanning Electron Microscope Fractography for D66 Tested at 232 °C (a) 200 x Magnification (b) 1000x Magnification.

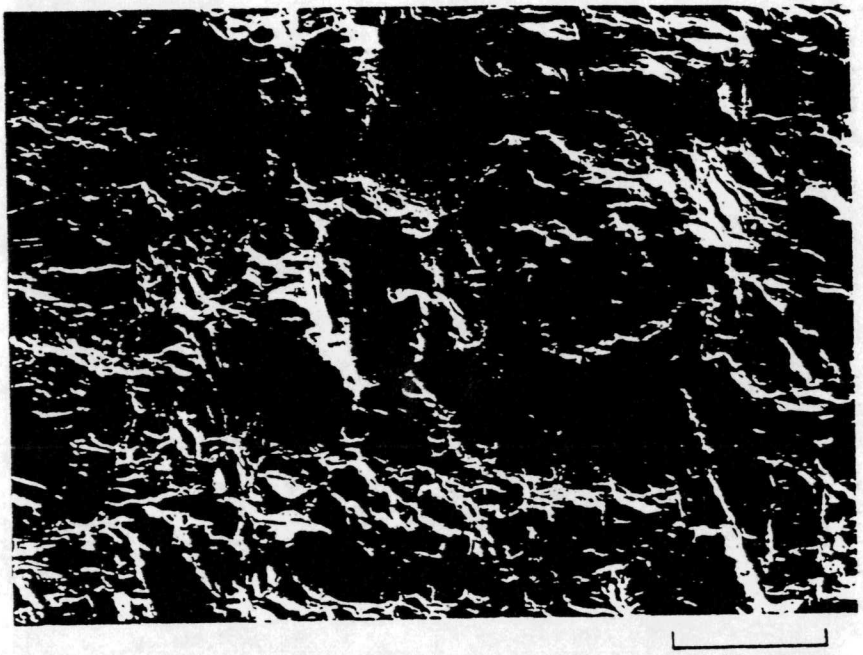

(a)

(b)

Figure 12. Scanning Electron Microscope Fractography for HT9 (a) Irradiated at 360 °C and Tested at 205 °C (b) Irradiated at 360 °C and Tested at 32 °C. 1000x Magnification.

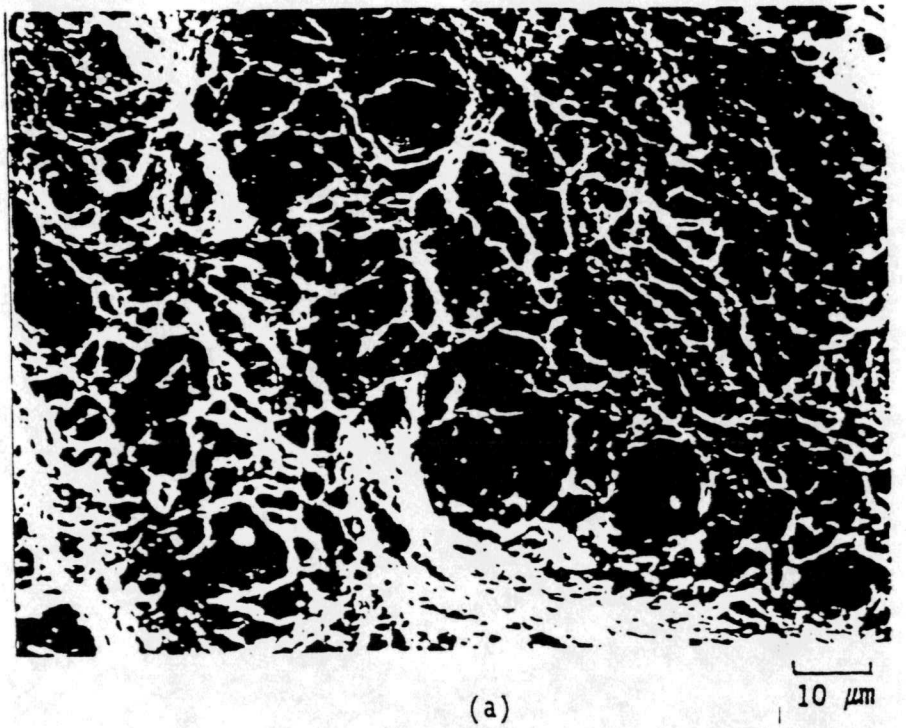

(a)

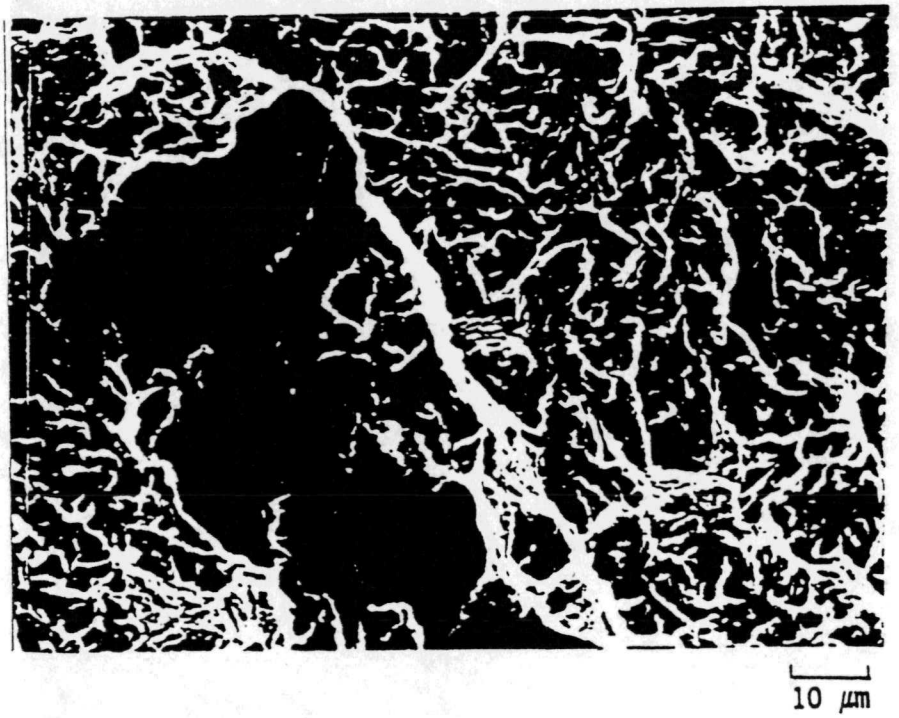

(b)

Figure 13. Fluence Dependence of K_c or K_{max} for Irradiated D9.

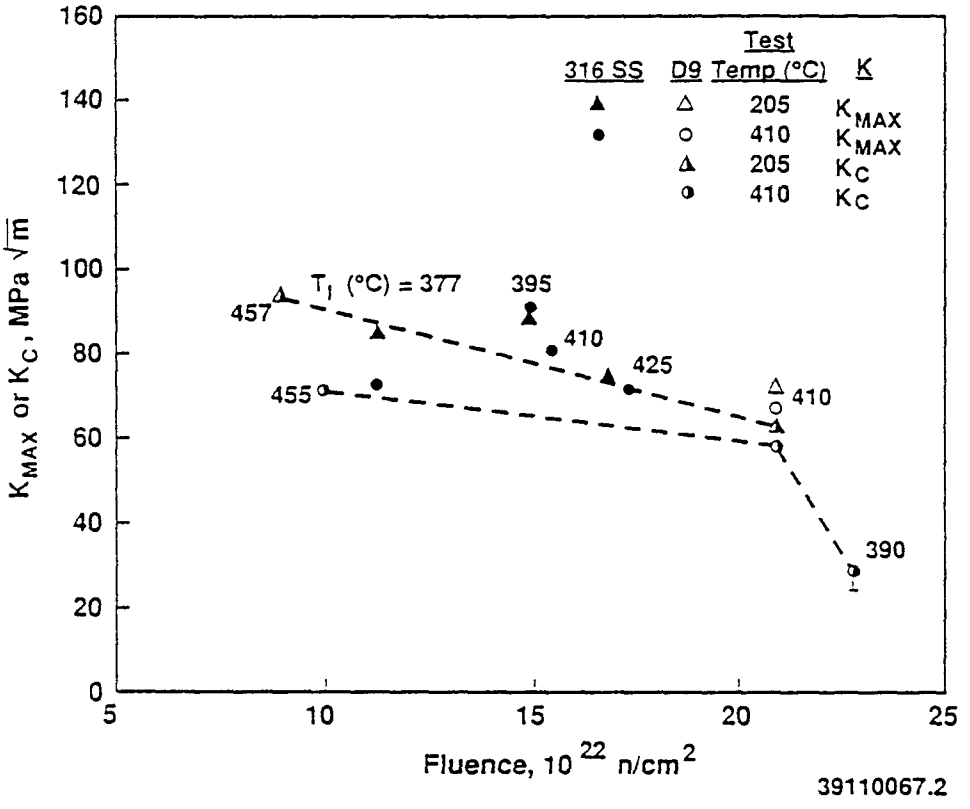

Figure 14. Fluence Dependence of K_c for Irradiated HT9.

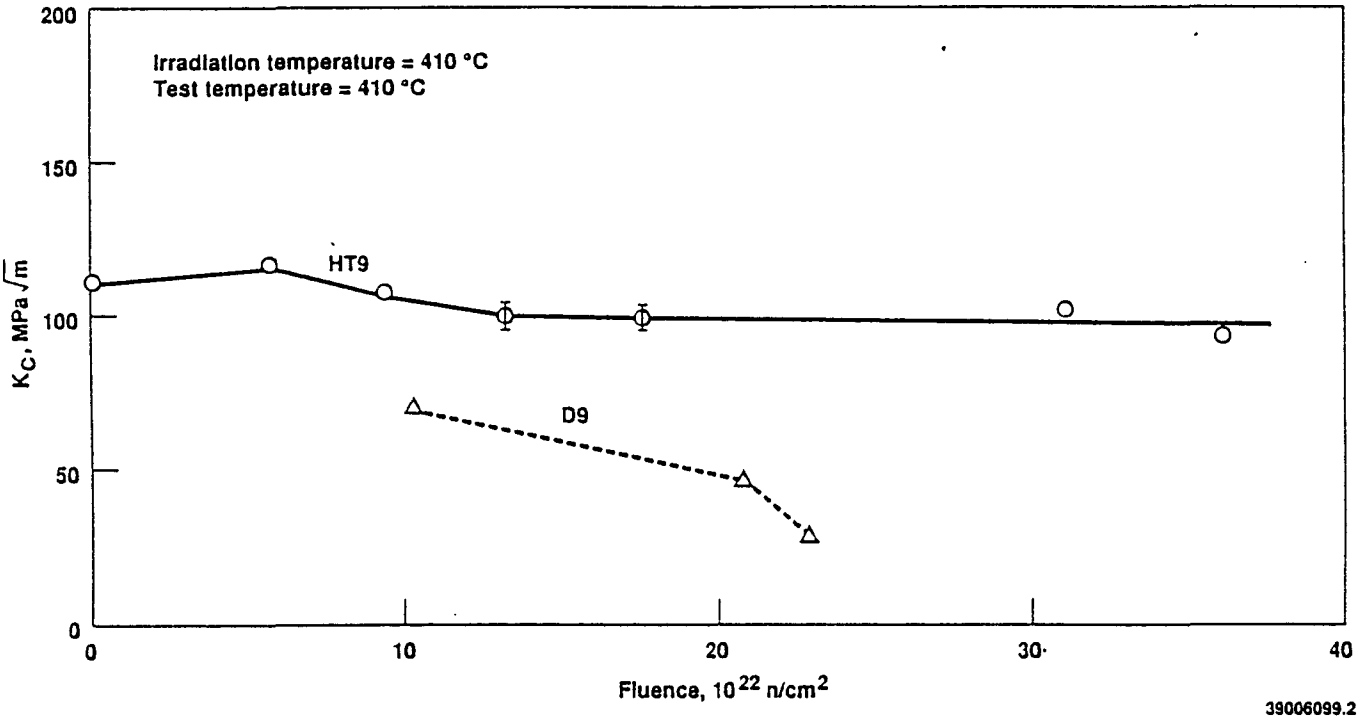

Figure 15. Fluence Dependence of Tearing Modulus for Irradiated HT9.

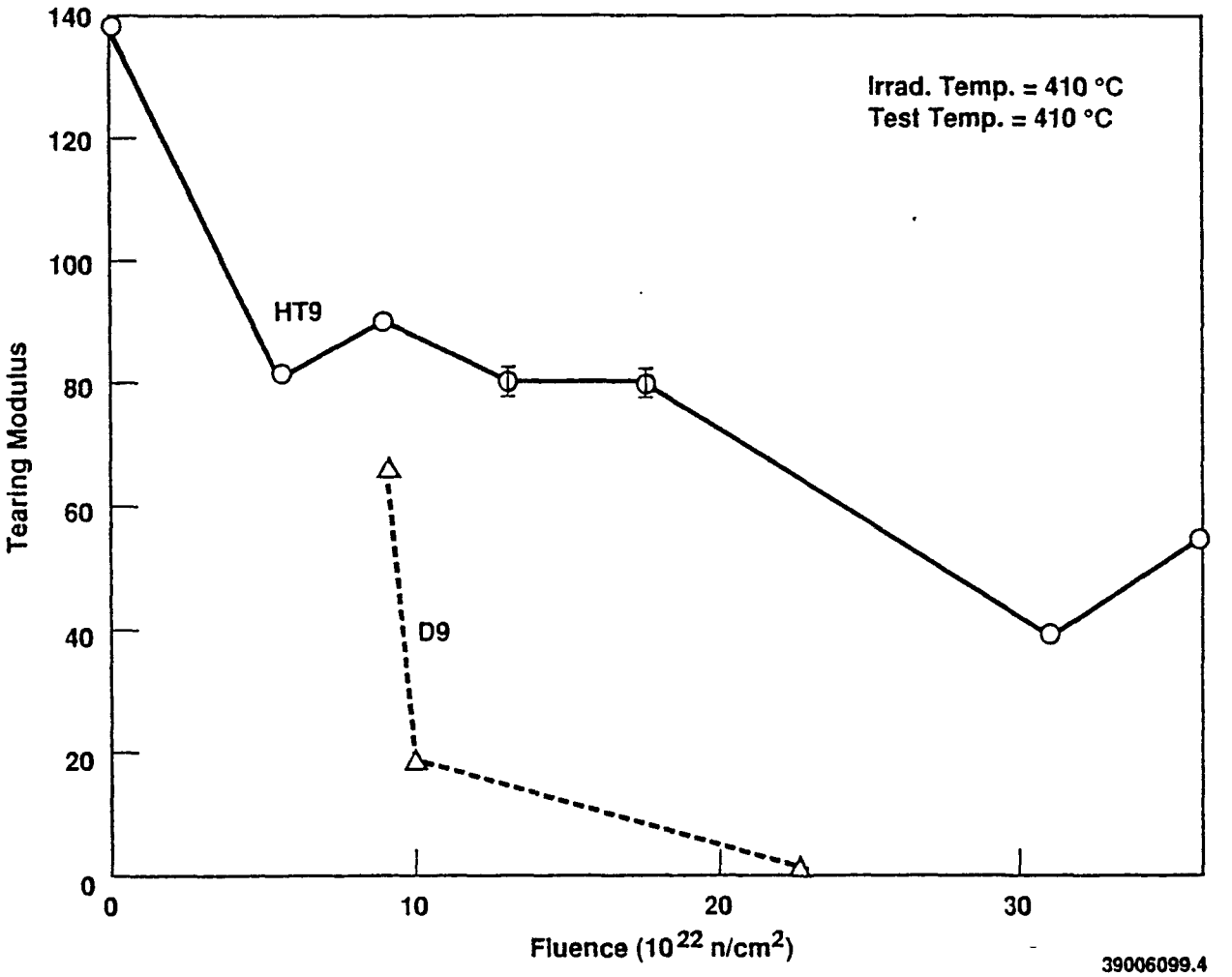

DISTRIBUTION

Number of copies

ONSITE

10

Westinghouse Hanford Company

W. F. Brehm	H5-67
F. H. Huang (2)	H5-67
Information Release Administration (2)	L8-07
Document Processing and Distribution	L8-15